Investigation of Fault Analysis for Renewable Energy Microgrid

**Afaneen A. Abbood[a]*, Hanan M. Habbi[b,c] , Mohamed A. Zohdy[c] **

[a]Communication Engineering Dept., University of Technology-Iraq, Alsina'a street, 10066 Baghdad, Iraq.

[b] Electrical Engineering Dept., University of Baghdad, Baghdad-Iraq.

[c] Electrical and Computer Engineering Dept., Oakland University Michigan, USA.
*Corresponding author Email: afaneen.a.abbood@uotechnology.edu.iq

H I G H L I G H T S

- The impact of all types of faults on system operation (islanded or grid-connected) was explored.
- The increment of the value of THD by 92% to 93.5% from its normal value indicates a fault occurrence.
- The value of the fault current specifies the type of protection system (fast or slow) in microgrid systems.

A R T I C L E I N F O

A B S T R A C T

This paper investigates the behavior of four bus grid-connected systems during different types of faults. The microgrid comprises a utility grid, a solar PV energy system, a diesel generator, and a load. Symmetrical and unsymmetrical faults at the microgrid distribution network were studied. These faults were applied at the solar PV bus under constant irradiance and temperature. The active and reactive power from the solar PV was synchronized based on the maximum power point tracking (MPPT) solar inverter. The total harmonic distortion (THD) for the load current response was also measured for each symmetrical and unsymmetrical fault. A protection system was strategically located based on specific constraints, such as fault location and detection. The simulation results were categorized into two scenarios: normal and abnormal conditions during faults in the distribution lines. The obtained results revealed significant differences in fault currents depending on the type of fault, which consequently influenced the selection of the appropriate protection system. The operation mode of the microgrid, whether in isolated or microgrid-connected mode, varied according to the fault type. Furthermore, the THD value of the load current exhibited a substantial increase during fault conditions. MATLAB/Simulink was utilized for conducting all the simulations.

1. Introduction

Due to the severity of the global energy crisis and concerns regarding increasing fuel prices and electrical shortages, there is a growing need for research in this field. Distributed generators and renewable energy resources such as solar and wind systems offer potential solutions. The microgrid plays a crucial role in managing power production within distribution systems by utilizing renewable energy resources connected to the power system. However, the significant integration of this renewable power source has started to impact the power system's stability, reliability, and quality. The negative effects on the power system must be addressed, including voltage fluctuation, voltage sag, harmonics, voltage flicker, power factor variations, and voltage imbalances at the point of common coupling (PCC). Consequently, several countries have adopted international standards grid codes to enforce stricter technical requirements for integrating renewable energy resources, aiming to ensure that no bad quality is injected into the grid. Moreover, renewable energy resources are expected to behave like traditional power plants and provide grid support during disturbances [1-5]. In a microgrid, fault analysis presents challenges due to the rapid increase in current during a fault [6,7]. Previous references have discussed various challenges, including frequency control, power quality, reactive power support, fault analysis, electricity market penetration, and environmental concerns. Wan et al. [8], proposed a rapid diagnosis technology for short-circuit faults in a DC microgrid, focusing on fault classification and location. Similarly, Nahas et al. [9], presented a fault analysis of a DC microgrid, considering the representation of its components. The microgrid included a solar PV system, batteries, and constant power loads. Abdul-Hamza and Habbi [10], investigated the detection and classification of fault types in the transmission power system, utilizing artificial neural networks, specifically backpropagation. A multiagent-based fault-current limiting scheme for microgrids was presented in. Chanbari and farjah work [11]. Simic et al. [12], focused on analyzing fault currents in two modes of operation within a microgrid, investigating improvements in fault calculations, and

analyzing relay protection. Prabha and Malviya [13], an analysis of cable faults in PV systems was presented, considering both L-G and L-L faults. Guo et al. [14], studied the value of HTF using αβ -frame impedance models of the droop inverters in islanded microgrids considering unbalanced loads. Jha et al. [15], presented a multifunction control model for a bidirectional interlinking converter (ILC) of renewable energy using an ac–dc hybrid microgrid. Mahmood and Michaelson work [16], a power management scenario for a PV battery hybrid system for islanded microgrids is proposed. Mohamed and Habbi [17] used a dual two-level inverter to minimize current signal total harmonic distortion (THD) for an open-end winding induction motor. C. Jiang and Z. Xia [18], proposed a fault detection and analysis method in microgrid systems using big data combing short-circuit current and voltage was presented. Mao et al. [19], a fault model and control structure of distributed generation sensor faults in an island microgrid was analyzed. The work in [20], proposed the implementation of a PV system with a micro-grid to improve the performance of the system considering large outages in Karbala city. In contrast Mohammed et al. [21], proposed a design of a 1MW grid-connected PV system for an Iraqi power system. The work considered solar radiation, technical design, system losses, environmental impact, and economic evaluations. Sumanth et al. [22], studied the analyses and presented the DC microgrids protection system using a ring configuration circuit. Mohamed and Habbi [17], presented a Photovoltaic panels system for powering the 3-phase Induction Motor.

The principal purpose of this paper was to study the fault effects on a microgrid. The three-bus microgrid system, including a utility generator, diesel generator with a transformer, AC (RL) load, and solar PV, has been modeled as shown in Figure 1. A PV solar array with MPPT boost dc to dc converter and connected to the microgrid by a Sinusoidal Pulse Width Modulation (SPWM) solar inverter. The main challenge constraints of faulty microgrids are power quality, total harmonic distortion, short circuit analysis, and protection systems. Regarding these constraints, different types of faults have been considered and tested in the simulation work. These faults include symmetrical and unsymmetrical faults, single and three-phase faults, and short circuit faults tests have been considered. The irradiance and temperature of $1000W/m^2$ and $25°C$ are kept constant. The maximum power point tracking based on perturb and observe algorithm is given in Aladely and Habbi [3]. The switching frequency of the inverter is 10 kHz.
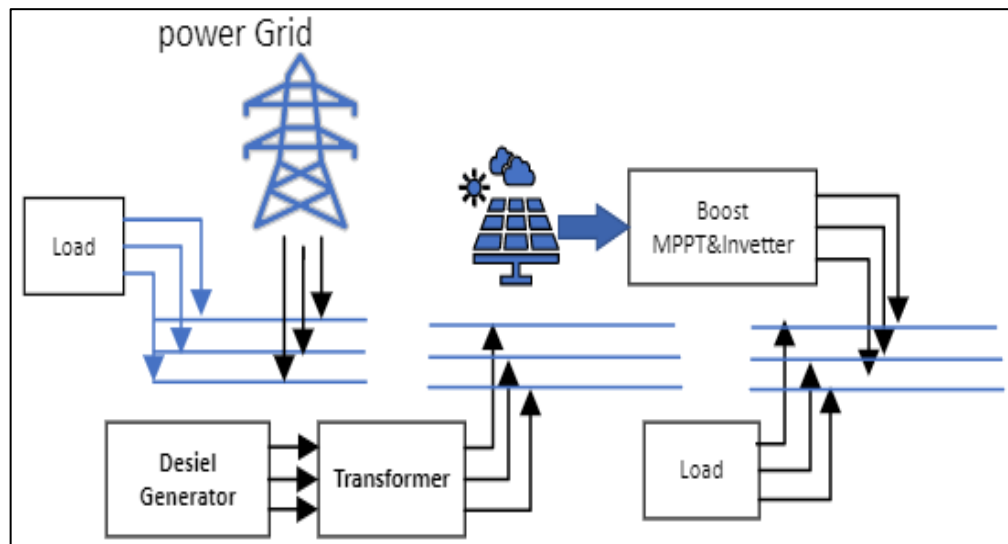

Figure 1: Microgrid system diagram

Under a fault scenario, most protection systems detect and diagnose based on grid parameter information. This information about the protection system is studied for results obtained for certain short circuit faults [10]. When a fault occurs in a DC microgrid, we do not need to estimate the system parameters to detect the fault, but it is difficult to distinguish the faulty line [23].
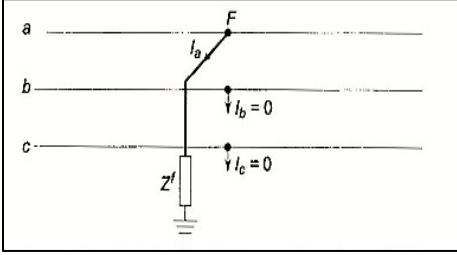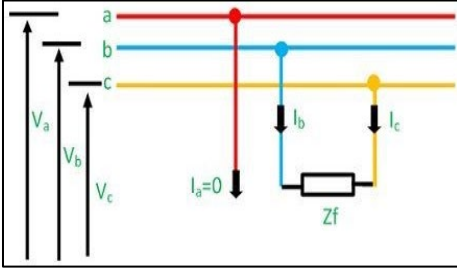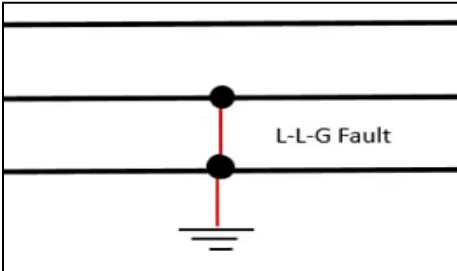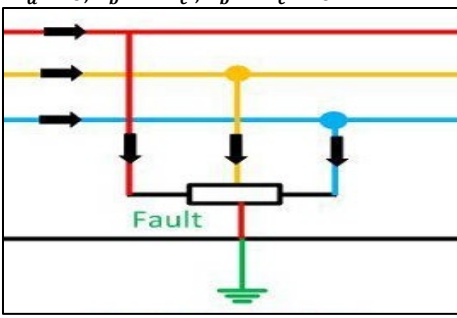
2. Faults Mathematical Representation

The most important challenges facing the electrical engineer are faults in the electrical transmission line system. Transmission line faults are caused by temporary disturbances such as lightning, conductor swings, trees, etc. For any utility company, service continuity is very important. Therefore, increased attention has been given to developing fast and accurate fault detection methods. Any protective system's intermediate stage before fault detection and classification is vital. The main types of fault are symmetrical and unsymmetrical faults, as below:

- Unsymmetrical faults which includes: Single line-to-ground (LG), Line-to-line (LL), Double line-to-ground (LLG)
- Symmetrical fault, which includes: Three phases to ground (LLLG)

The most common fault in the power distribution network is the line-to-ground fault (LG), while the most severe fault is the three-phase to-ground [24].

The mathematical representation of the above types of faults is tabulated in Table 1.

Table 1: Mathematical representation of the different fault types

Single line to ground fault	
	$I_b = I_c = 0$
Line-to-line fault	
	$I_a = 0,\ I_b = -I_c\ ,V_b = V_c$
Double line to ground fault	L-L-G Fault
	$I_a = 0,\ I_b = -I_c\ ,V_b = V_c = 0$
Three line to ground fault	Fault
	$V_a = V_b = V_c = 0$

All the above types of faults were taken into consideration in this paper.

3. Microgrid Model

This work has developed and simulated four bus microgrid systems, including a utility generator, a diesel generator with a transformer, two AC (RL) loads systems, and solar PV, with MATLAB/Simulink. The 400 V, 50 Hz distribution system has been selected. The MATLAB/Simulink of the proposed system is indicated in Figure 2. It can be observed that the utility grid is connected to bus 1. The AC load is tied to Bus 2, the solar PV system is connected to Bus 3, and the diesel generator is connected to Bus 4. The distribution line parameters of R=0.02Ω and X_L= 0.025Ω have been set. A 10 MW Y/D transformer is used for the diesel generator. The diesel generator acts as an additional power generator to balance the power generation and the load demands. A 3-phase circuit breaker is used to control the breaking of the load. At the same time, a 3-phase fault block is expended to implement different types of faults on the microgrid.

The load of 5 MW and 10MVAR has been loaded in the microgrid. A fault block is placed in each bus to analyze the effects of the faults on the proposed system.
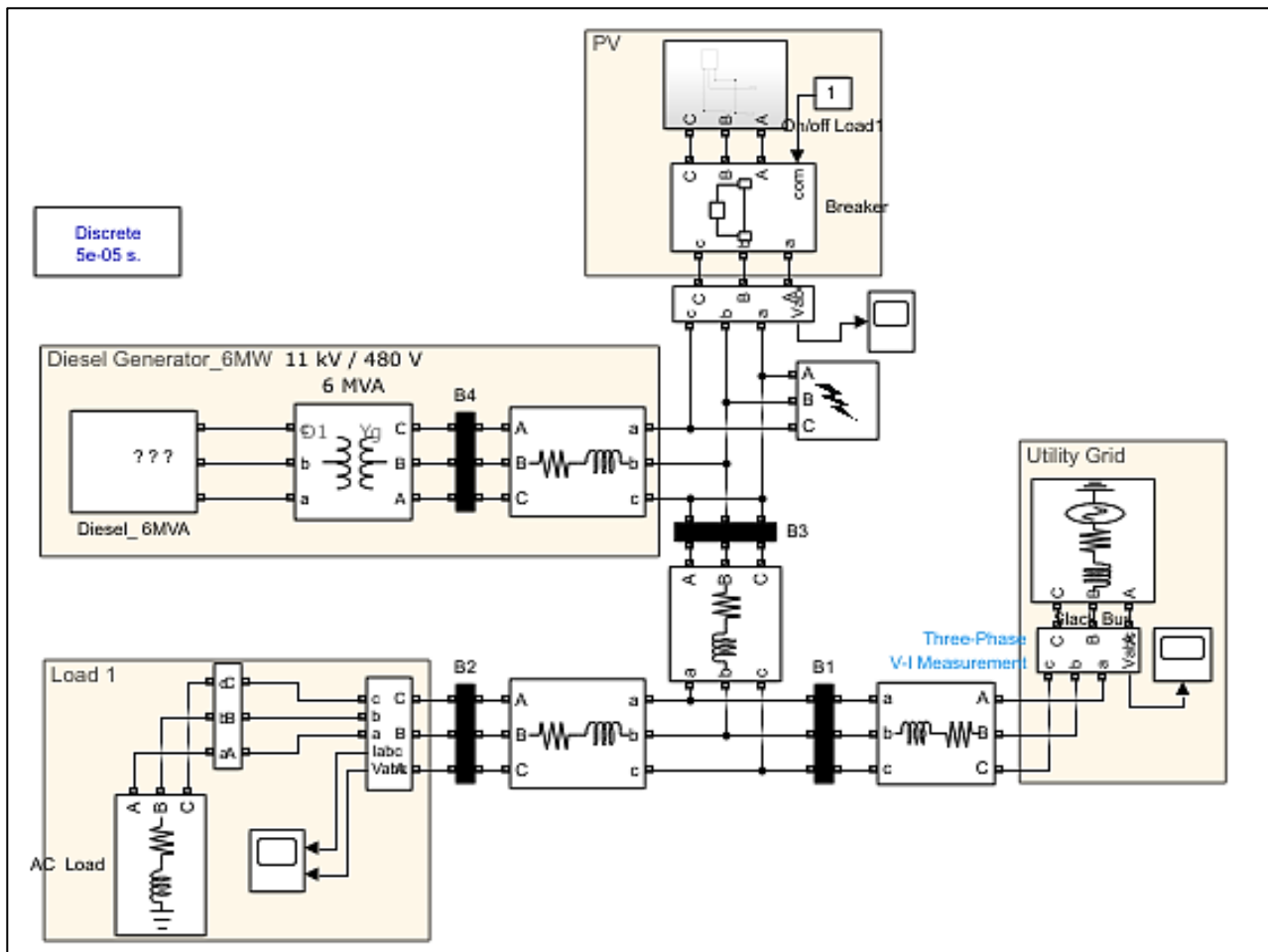
Figure 2: MATLAB/Simulink diagram for the proposed system with load

3.1 PV Solar Model

The specification of the PV panel is SunPower SPR-305E-WHT-D, the number of parallel strings (Np) is 20, and the number of series-connected modules per string (Ns) is 10. The PV array is designed for 6 MW. The irradiance and temperature curve for the PV panel is shown in Figure 3. Hence, the system adopted one day as the irradiance of 1000 W/m² at a temperature of 25℃. The equivalent circuit of the solar cell is indicated in Figure 4. The solar PV system is based on Perturb & Observe (P&O)-MPPT. The P&O MPPT MATLAB program is given in Appendix A [21].
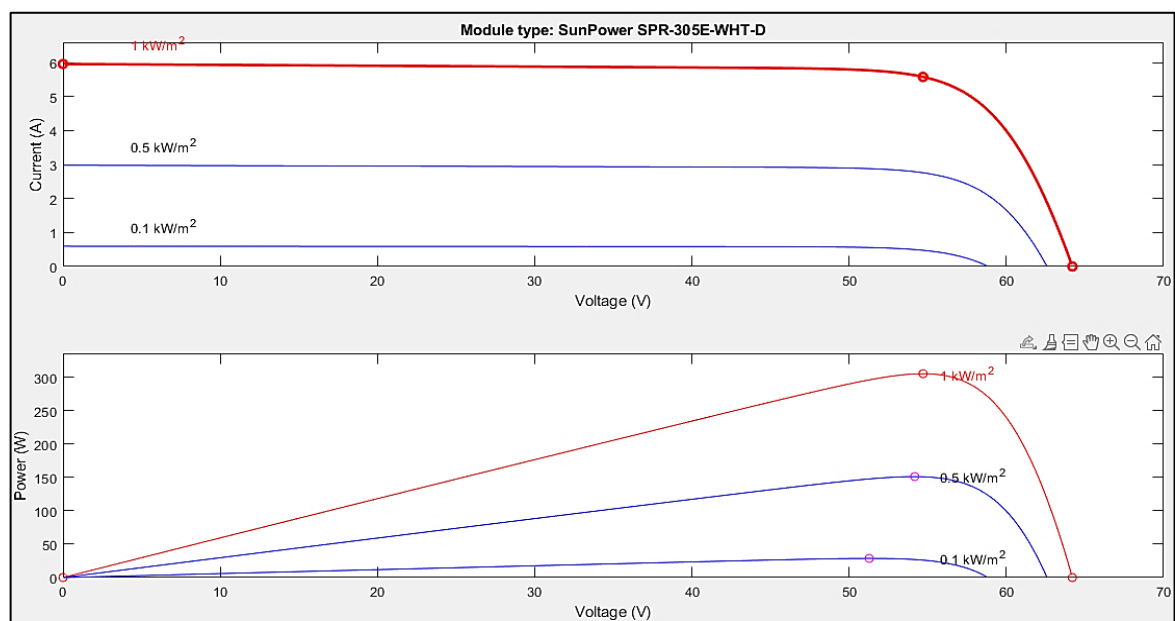

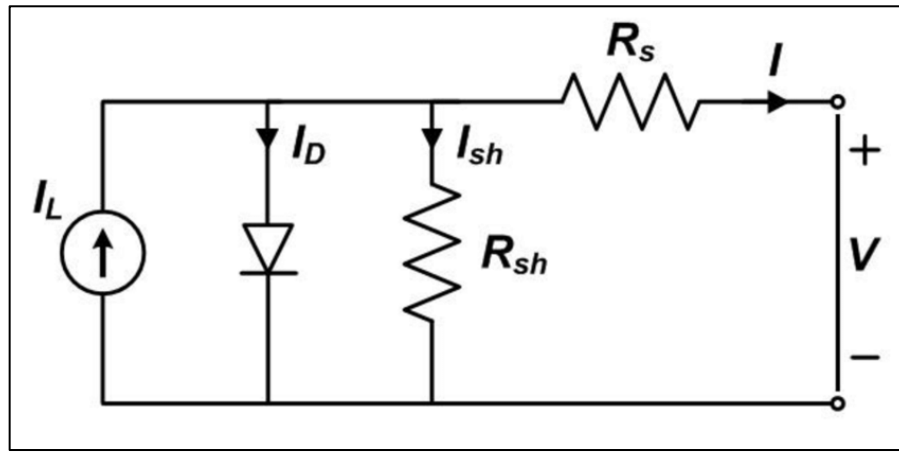**Figure 3:** Solar PV characteristics (IV curve and PV curve)

Figure 4: Equivalent circuit of the Solar Cell Module

As shown in Figure 4, the current of the PV cell (*I*) is given by Equation 1 as:

$$I = I_L - I_D - I_{sh} \tag{1}$$

The diode current (ID) is

$$I_D = I_o[e^{\frac{(V-IR_S)}{nV_T}} - 1] \tag{2}$$

Where the output voltage is given by:

$$V = 1.381x10^{-23}J/K.\frac{T_c}{1.602x10^{-19}C} \tag{3}$$

The shunt current (I_{sh}) is

$$I_{sh} = \frac{V+IR_S}{R_{sh}} \tag{4}$$

Substitution Equations 2 and 4 in to Equation 1, gets Equqtion 5:

$$I = I_L - I_o\left[e^{\frac{(V-IR_{S)}}{nV_T}} - 1\right] - \frac{V+IR_S}{R_{sh}} \tag{5}$$

Figure 5 shows the MATLAB/Simulink block of the PV solar system.

A control circuit was implemented to simulate the switching pf the boost dc to dc converter in the solar system. To achieve synchronization between the V_{abc} output of the PV solar system's inverter and the grid, a phase-locked loop (PLL) was utilized, as depicted in Figure 6.
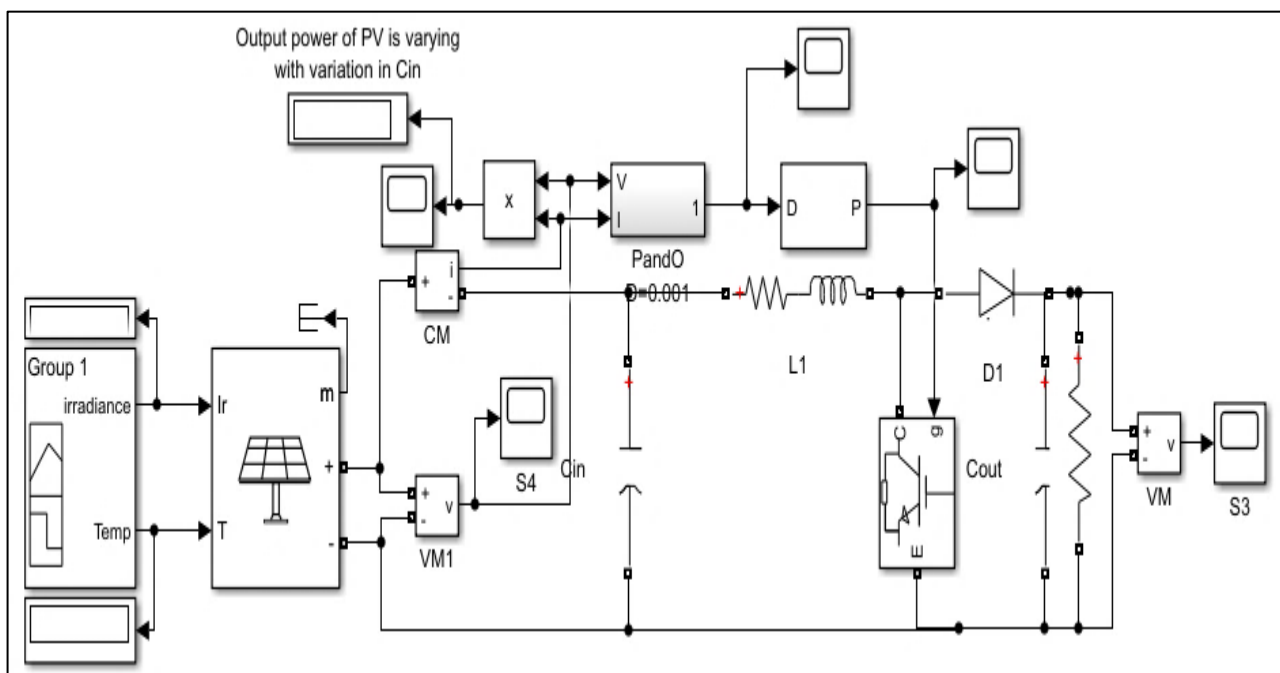

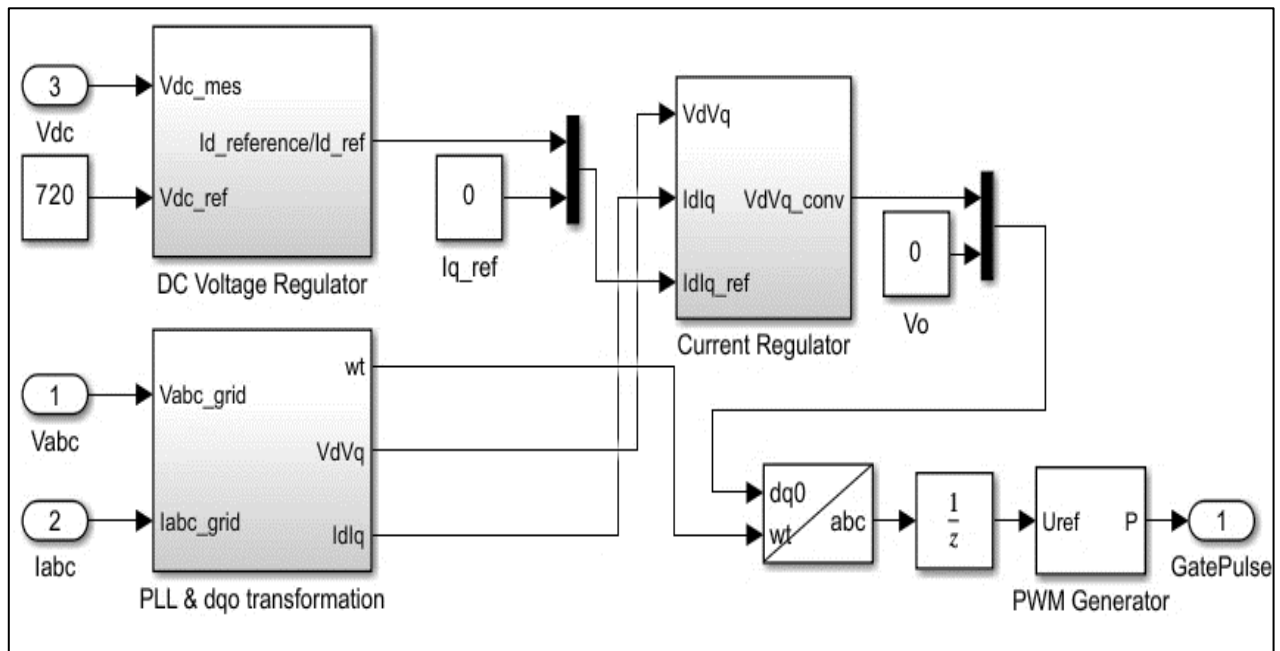**Figure 5:** PV solar MATLAB/Simulink model

Figure 6: Control circuit of the Solar PV, including PLL

3.2 Diesel Generator (DG) Model

The diesel generator (DG) model is illustrated in Figure 7 a,b. The DG is connected to bus 4 which has a specification of 6MW, with a 10MW power transformer of 11kV/400V. A Permanent Magnet Synchronous Generator (PMSG) is employed in the proposed model. The PMSG incorporates a synchronous machine voltage regulator and exciter based on the IEEE-type AC1A excitation system model.
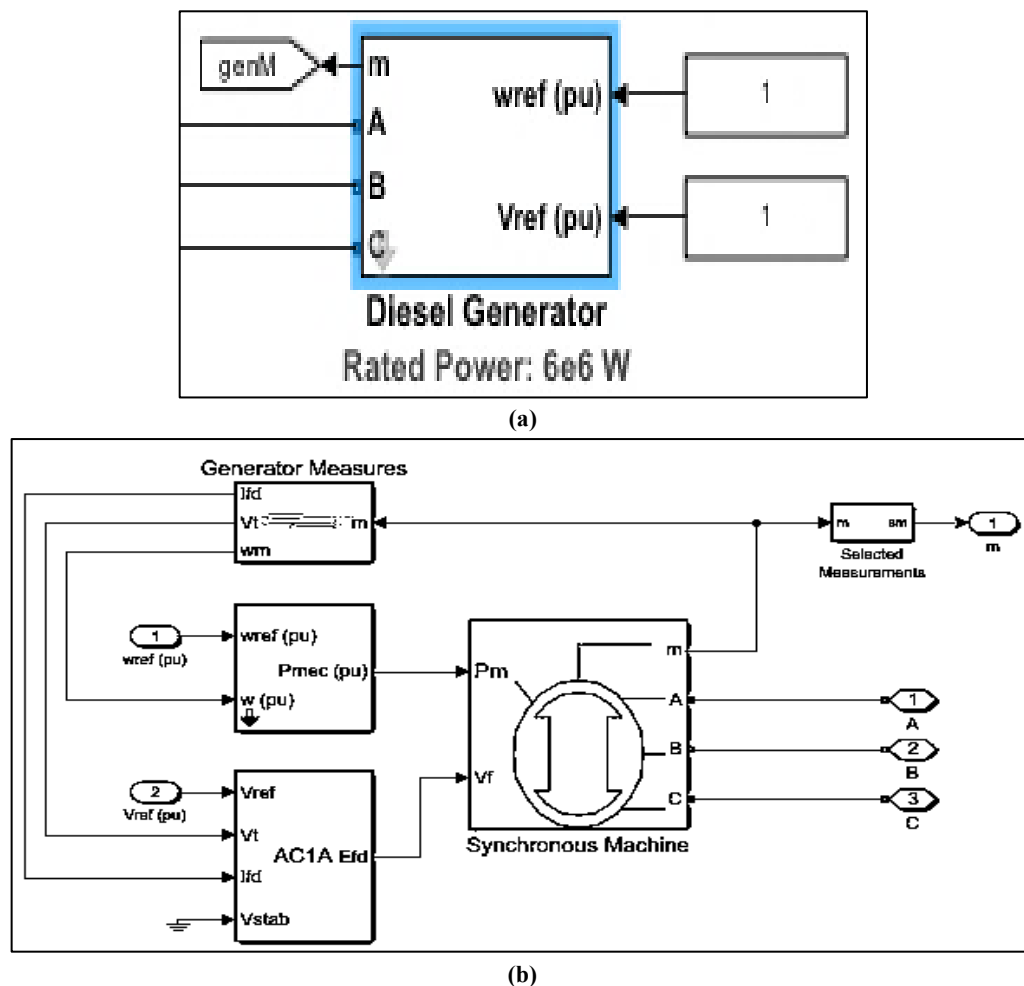

(a)

(b)

Figure 7: Diesel generator model:a) Diesel Generator Block, b) The construction model of the Generator

3.3 THD Model

Figure 8 shows the MATLAB/Simulink THD model. The high faulty current risks damaging the feeder cables and the power electronic devices within a short transient period. Therefore, it is crucial to isolate the microgrid promptly. To mitigate this issue, the total harmonic distortion (THD) is considered with a sampling time of 0.2 ms. The THD of the current signal can be calculated using Equation 6 [24]

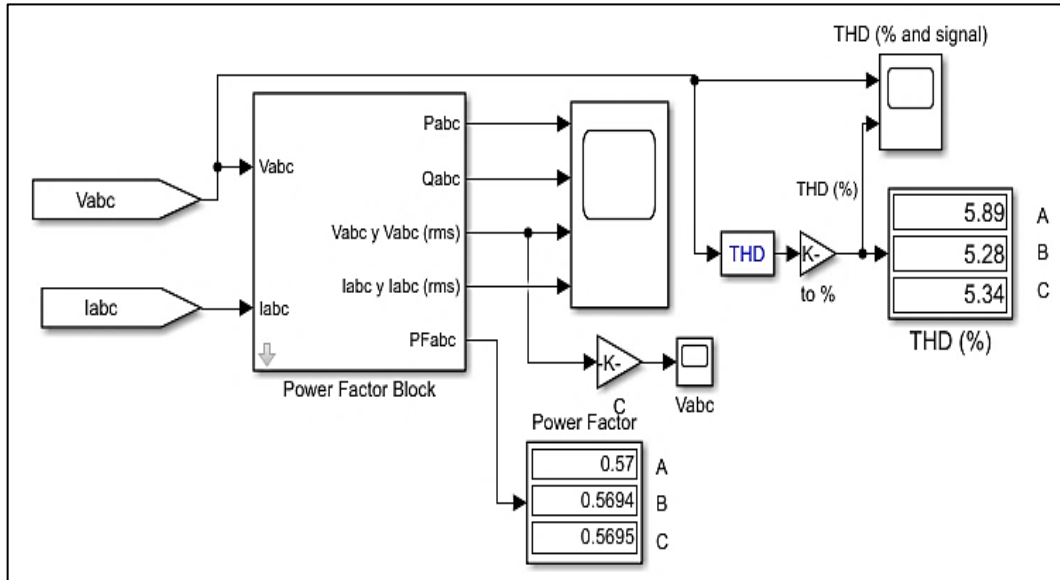$$\% \text{ current THD} = \frac{\sqrt{I_2^2 + I_3^2 + I_4^2 + I_N^2}}{I_1} \times 100 \tag{6}$$

Figure 8: THD Matlab/Simulink model

3.4 The Protection Model

Disturbances and load outages can lead to short-circuiting conditions [2]. The high value of short-circuit current through the equipment can cause damage and service disconnection. In a power system, the ratings of equipment and devices are chosen based on the short circuit current value. Therefore, there is an urgent need for highly efficient protection systems that can accurately detect faults. These protection systems are designed to sense faults occurring in any part of the power system, after which the circuit breaker is tripped. The MATLAB/Simulink diagram of the proposed protection system is depicted in Figure 9. If the current exceeds the rated value, a relay must send a warning to initiate the operation of the breaker, resulting in the isolation of faulty components from the system. In other words, when a fault occurs at bus 3, the microgrid will be isolated from the utility grid. For each type of fault, the current value must be monitored to determine whether the microgrid is operating in islanding or grid-connected mode. Circuit breakers are placed at different locations across the microgrid buses and must autonomously detect faults. A protection relay scheme is implemented to limit the short-circuit fault current during off-grid operation, ensuring high accuracy in security decisions with the assistance of circuit breakers.
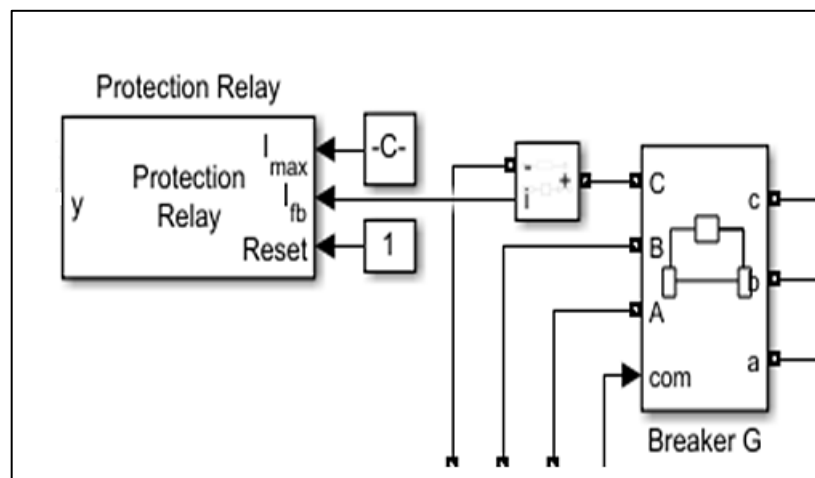

Figure 9: MATLAB/Simulink diagram for the proposed protection system

4. Simulation Results

The simulation results were obtained for different fault locations within the microgrid, considering both short-circuit symmetrical and unsymmetrical faults. The simulation results are categorized into two scenarios: normal and abnormal conditions during faults occurring on the distribution line between renewable energy bus 2 and utility grid bus 1. In the simulation, the fault current and the THD value were monitored to demonstrate the operational performance of the circuit breaker and the relay and their respective locations within the microgrid.

4.1 Scenario 1-Normal Condition

The simulation results of load voltages and currents under normal conditions in the microgrid are displayed in Figure 10. The voltage and current values remain within acceptable limits and the value of the THD is 1.49%.
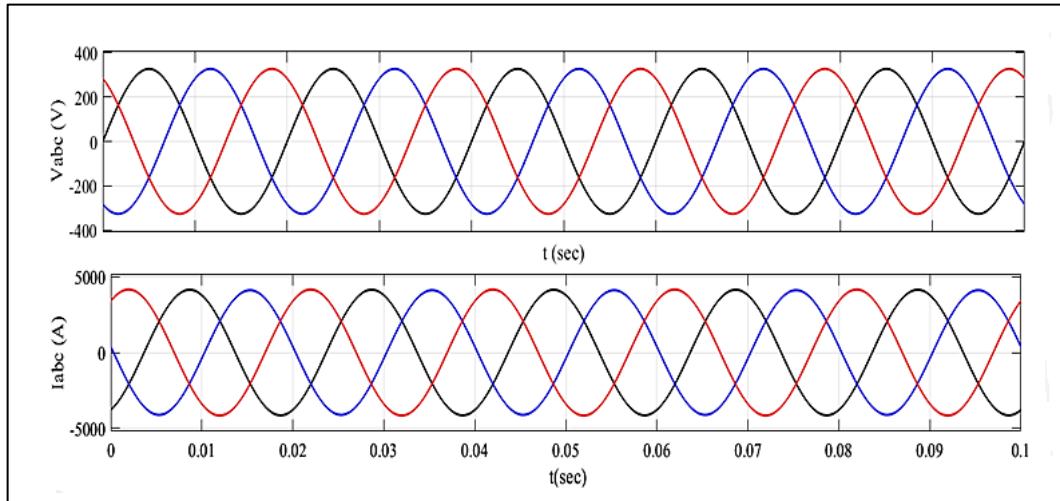

Figure 10: Load voltages and currents for the healthy condition

4.2 Scenario 2- Abnormal Condition

The simulation results of load voltages and currents in the microgrid are presented and categorized based on the types of faults that occurred specifically on the renewable energy line.

4.2.1 LG fault

Figure 11 illustrates the simulation results for the current signal during an LG fault. The current passes through the faulted phase, resulting in noticeable distortion. As depicted in Figure 11, the current in the faulty phase decays to a low value at t=0.085 sec. Furthermore, the total harmonic distortion (THD) value is 19.88%.
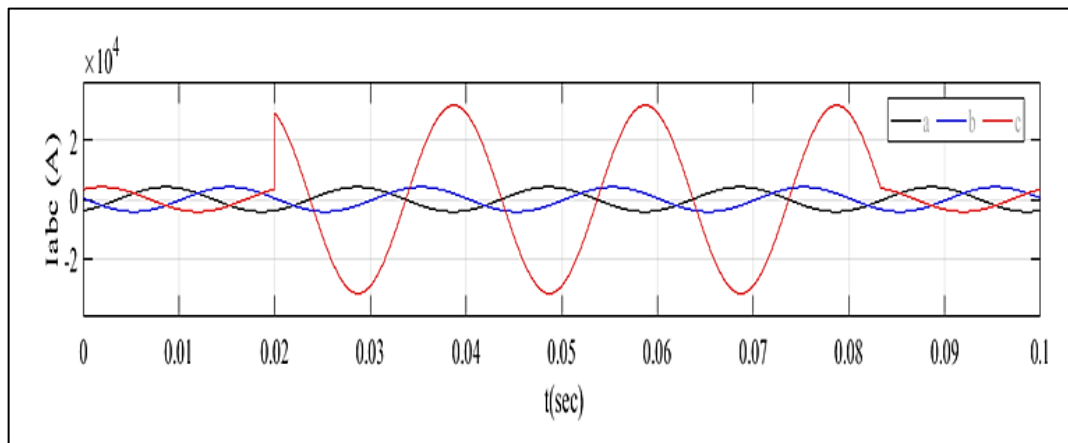

Figure 11: Fault currents at LG fault

4.2.2 LL fault

Figure 12 displays the simulation results for the current signal during an LL fault. The currents in the faulty phases reach high values, indicating a short-circuit current. The line impedances influence the magnitude of the fault currents. It can be inferred that a fault occurring at a distant location from the energy generator source will not significantly impact the fault current compared to the rated current. As a result, there is no need to utilize fast protection components in such scenarios. Conversely, when the fault current is high, fast protection components are necessary, on the other hand, the value of the THD value is 20.86%.
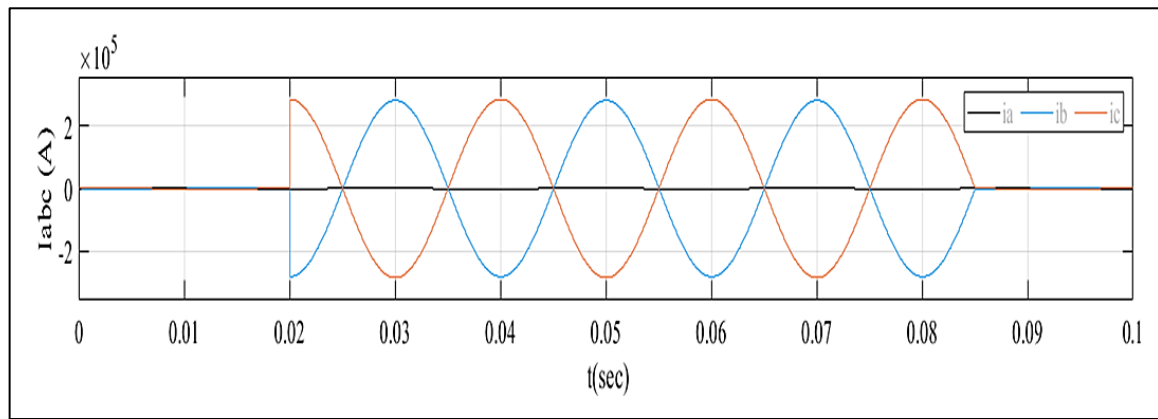
Figure 12: Fault currents at LG fault

4.2.3 LLG fault

Figure 13 depicts the simulation results for the load currents during an LLG fault. It is evident that the current in the faulty phases experiences distortion. The load current exhibits a high value at the moment of fault occurrence (t=0.02s). The total harmonic distortion (THD) for the load current is 22.5%.

4.2.4 LLLG fault (Off - Grid)

Figure 14 displays the simulation results for the load currents during an LLLG fault. It is evident that the current in the faulty phases experiences distortion. The measured total harmonic distortion (THD) is 22.75%. The fault occurs at t=0.02 sec and is cleared at t=0.087 sec, after which the system operates properly. This fault is considered a worst-case scenario, as the current transformers may need to handle high fault currents. Typically, the current transformers are designed to handle short circuit currents up to 20 times their rating, depending on the load demand.
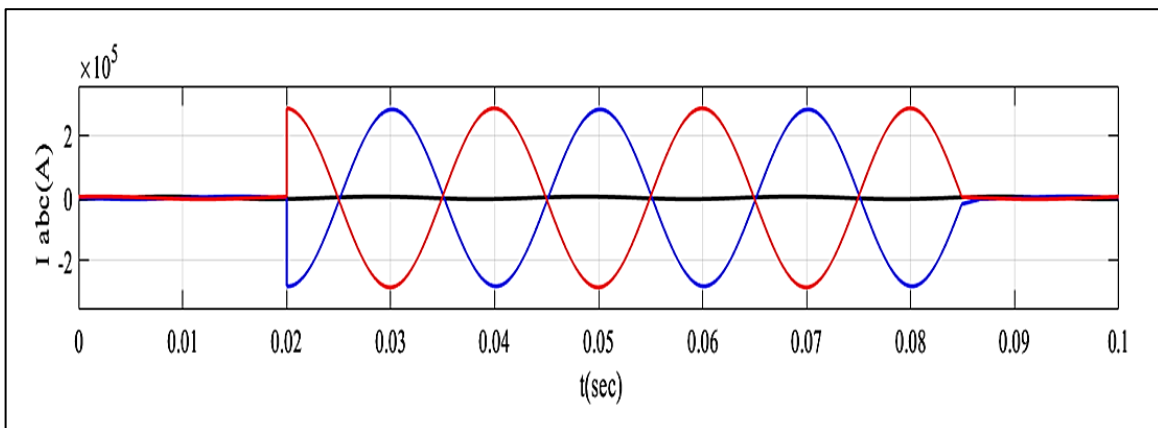

Figure 13: Load currents at LLG fault

Figure 14: Load currents at LLLG fault
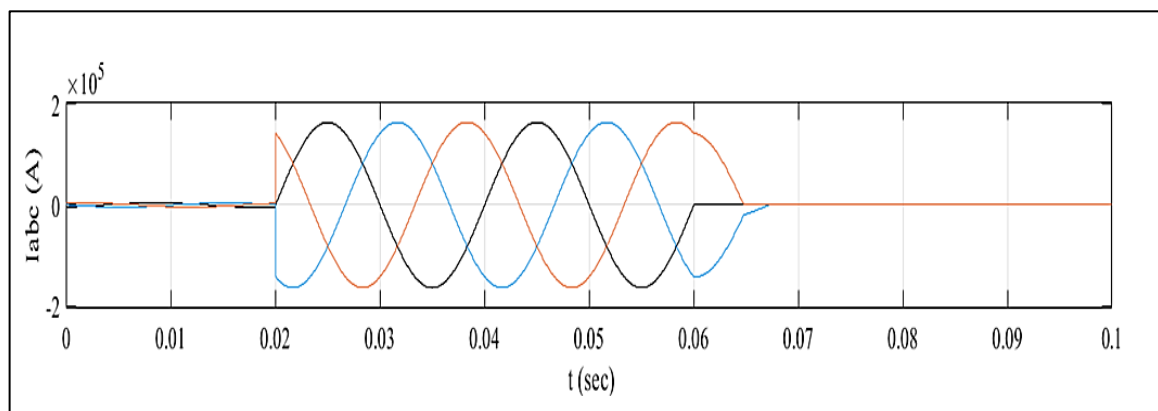
From Figure 14, it can be concluded that the fault currents have a high magnitude, indicating the need for fast protection. The fault identification is achieved through trial and error, followed by its isolation from the faulty distribution network. The simulation results also indicate that the fault occurred at t=0.02 sec and was cleared at t=0.06 sec, confirming the successful

operation of the proposed protection control in terms of fault identification and isolation. Therefore, fast protection components are necessary for such high current faults.

Table 2 presents the tabled values for THD for each fault type. It is evident that when the THD value exceeds the normal range of 1.49% (ranging from 92.5% to 93.5%), it indicates a fault in a specific line of the microgrid.

Furthermore, based on the obtained results, it can be concluded that the microgrid operates in island mode during an LLLG fault, while it remains in grid-connected mode during other faults.

Table 2: THD according to Types of faults

Type of fault	symbol	THD%
Healthy system	-	1.49
line to ground	LG	19.88
line to line	LL	20.86
double line to ground	LLG	22.5
Three phases to ground fault	LLLG	22.75

5. Conclusion

In this paper, a study on fault analysis in microgrid operations was conducted. The simulated microgrid model included a renewable solar PV generator system with constant irradiance and temperature, a diesel generator, a utility grid, and loads. Various types of short-circuit symmetrical and unsymmetrical faults were considered. The impact of fault occurrence on the microgrid's mode of operation, whether in off-grid or grid-connected mode, was discussed. The study also examined total harmonic distortion (THD) and the selection of appropriate protection measures. The main objectives of feeder protection in a microgrid are to identify different fault types and swiftly clear them to prevent equipment damage.

The results showed that symmetrical faults generate the highest fault current, necessitating fast protection systems for fault detection. Conversely, other fault types do not require fast protection. The analysis of the THD of the load current signal, as presented in Table 2, demonstrated that an increase in THD by 92% to 93.5% from its normal value can indicate a fault in the microgrid. Additionally, the mode of operation, whether isolated or grid-connected, varies depending on the fault type. It was observed that the system operates in island mode during the occurrence of symmetrical faults (LLLG), while it remains in the grid-connected mode for other fault types. Future research challenges include studying variable irradiance and temperature conditions for solar PV systems and exploring minimum frequency fluctuations during fault occurrences in microgrids.

Appendix A
P&O M-file code
```
function y = fcn(u,i,uo,io,D)
m=0;
du=u-uo;
di=i-io;
dp=(u*i)-(uo*io);
d=.001;
if dp>0
    if du>0
        m=D+d;
    else
        m=D-d;
    end
else
    if du>0
        m=D+d;
    else
        m=D-d;
    end
end
y = m;
end
```

Author contributions

Conceptualization, A. Abbood. H. Habbi. and M. Zohdy; methodology, A. Abbood; software, A. Abbood;validation, A. Abbood. H. Habbi. and M. Zohdy; formal analysis, A. Abbood; investigation, A. Abbood; resources, A. Abbood; data curation, A. Abbood; writing—original draft preparation, A. Abbood; writing—review and editing, A. Abbood; visualization, A. Abbood; supervision, A. Abbood; project administration, A. Abbood. All authors have read and agreed to the published version of the manuscript.

Conflicts of interest

The authors declare that there is no conflict of interest.

References

[1] D. Park and M. Zadeh, Dynamic Modeling, Stability Analysis, and Power Management of Shipboard DC Hybrid Power Systems, IEEE Trans. Transp. Electrif., 8 (2022) $225-238$. https://doi.org/10.1109/TTE.2021.3119231

[2] N. Kumar, B. Singh and B. K. Panigrahi, Grid synchronization framework for partially shaded solar PV-based microgrid using intelligent control strategy, IET Gener. Transm. Distrib., 13 (2019) 829-837.https://doi.org/10.1049/iet-gtd.2018.6079

[3] A. Aladely and H. M. D.Habbi, Design and Performance Analysis of a 3-phase Induction motor for Solar Photovoltaic fed Pumping System, J. Eng. Appl. Sci., 15 (2020) 773-782. https://dx.doi.org/10.36478/jeasci.2020.773.782

[4] H. M. Dawood Habbi, Genetic Controller Stator-Flux Orientated Vector Control of Doubly-Fed Induction Generator for Wind Power Generation System, Int. J. Comput. Appl. Technol., 179 (2018) 28-32. http://dx.doi.org/10.5120/ijca2018916324

[5] A. M. Abdul Hussain and H. M. D. Habbi, Maximum Power Point Tracking Photovoltaic Fed Pumping System Based on PI Controller, IEEE Conf. 2018 3rd Sci. Conf. Electr. Eng., 78-83, 2018. https://doi.org/10.1109/SCEE.2018.8684120

[6] T. Chia Ou, A novel unsymmetrical faults analysis for microgrid distribution systems, Int. J. Electr. Power Energy Syst., 43 (2012) 1017-1024. https://doi.org/10.1016/j.ijepes.2012.05.012

[7] Z. Zhang, Q. Chen, R. Xie, K. Sun, The Fault Analysis of PV Cable Fault in DC Microgrids , IEEE Trans. Energy Convers., 34 (2019) 486-496. https://doi.org/10.1109/TEC.2018.2876669

[8] Q. Wan, S. Zheng, C. Shi, A rapid diagnosis technology of short circuit fault in DC microgrid, Int. J. Electr. Power Energy Syst., 147 (2023) 108878. https://doi.org/10.1016/j.ijepes.2022.108878

[9] E. W. Nahas, H. A. Abd el-Ghany, D. A. Mansour, M.M. Eissa, Extensive analysis of fault response and extracting fault features for DC microgrids&z.star, Alexandria Eng. J., 60 (2022) 2405-2420. http://dx.doi.org/10.1016/j.aej.2020.12.026

[10] A. A. Abdul-Hamza and H. M. Habbi, Fault detection and diagnosis based on artificial neural network, Int. J. Sci. Eng. Res., 7 (2016) 1690-1697.

[11] T. Chanbari, and E. farjah, A Multiagent-based Fault Current Limiting Scheme for the Microgrids, IEEE Trans. Power Delivery., 29 (2014) 525-533. http://dx.doi.org/10.1109/TPWRD.2013.2282917

[12] N. Simic, L. Strezoski, B. Dumnic, Short-Circuit Analysis of DER-Based Microgrids in Connected and Islanded Modes of Operation, Energies, 14 (2021) 6372. https://doi.org/10.3390/en14196372

[13] R. Prabha, R. Malviya, Design and Fault analysis of Photovoltaic Cable Array with Grid Connected Systems, J. Emerging Technol. Innovative Res., 8 (2021) 765-770.

[14] J. Guo, Z. Meng, y. chen, W. Wu, S. Liao and Z. Xie, harmonics transfer function based frame SISO impedance modeling of droop inverters-based islanded microgrid with unbalanced loads, IEEE Trans. Ind. Electron., 70 (2023) 452-464. https://doi.org/10.1109/TIE.2022.3156043

[15] S. Jha, B. Singh, and S. Mishra, Control of ILC in an Autonomous AC-DC hybrid microgrid with unbalanced nonlinear AC loads, IEEE Trans. Ind. Electron., 70 (2023) 544-554. https://doi.org/10.1109/TIE.2022.3148754

[16] H. Mahmood and D. Michaelson, A Power Management Strategy for PV/Battery Hybrid Systems in Islanded Microgrids, IEEE J. Emerging Sel. Top. Power Electron., 2 (2014) 870 - 882. https://doi.org/10.1109/JESTPE.2014.2334051

[17] H. A. Mohamed and H. M. D. Habbi, Power quality of dual two-level inverter fed open end winding induction motor, Indones. J. Electr. Eng. Comput. Sci., 18 (2020) 688- 697. http://dx.doi.org/10.11591/ijeecs.v18.i2.pp688-697

[18] C. Jiang and Z. Xia, Application of a Hybrid Model of Big Data and BP Network on Fault Diagnosis Strategy for Microgrid, Comput. Intell. Neurosci, 2022 (2022)1-12. https://doi.org/10.1155/2022/1554422

[19] J. Mao, C. Yin, X. Zhang, A. Wu, and X. Zhang, Learning Observer-Based Sensor Fault-Tolerant Control of Distributed Generation in an Islanded Microgrid for Bus Voltage Sta bility Enhancement, Sensors, 22 (2022) 6907. https://doi.org/10.3390/s22186907

[20] A. A. Abbood, M. A Salih and A. Y Mohammed, Performance Improving of Grid Connected Photovoltaic System with Grid Contain Heavily Outages, Int. J. Curr. Eng. Technol., 7 (2017) 1950- 1957.

[21] A. Y. Mohammed, A. A. Abbood and M. A. Salih, Modeling and simulation of 1MW grid connected photovoltaic system in Karbala city, Int. J. Energy Environ., 9 (2018)153-168.

[22] Sumanth, A. Srivastava, S. Modi, Fault Analysis and Protection of DC Microgrid, Int. J. Eng. Res. Technol., 8 (2020) 122-126. https://doi.org/10.17577/IJERTCONV8IS1102810

[23] A. A. Abbood and R. A. Abttan, Multiple Fault Detection, Classification and Location in Electric PowerTransmission Lines in Matlab Environment, Int. J. Eng. Technol., 7 (2018) 111-119.

[24] S. K. Prince , S. Affijulla and G. Panda, Total Harmonic Distortion based Fault Detection in Islanded DC Microgrid, 2020 3rd Int. Conf. Energy, Power and Environment: Towards Clean Energy Technologies, Shillong, Meghalaya, India, 2021, 1-6. https://doi.org/10.1109/ICEPE50861.2021.9404407